Scripta Materialia 154 (2018) 87–91

Contents lists available at ScienceDirect

Scripta Materialia

journal homepage: www.elsevier.com/locate/scriptamat

Regular article

In-situ observation of an irradiation creep deformation mechanism in zirconium alloys

M. Gaumé [a], P. Baldo [b], F. Mompiou [c], F. Onimus [a,*]

[a] DEN, Service de Recherches de Métallurgie Appliquées, CEA Saclay, Université Paris-Saclay, F-91191 Gif-sur-Yvette, France
[b] Materials Science Division, Argonne National Laboratory, Argonne, IL 60439, United States
[c] CEMES-CNRS, Université de Toulouse, 29 Rue Jeanne Marvig, 31055 Toulouse Cedex 4, France

ARTICLE INFO

Article history:
Received 18 April 2018
Received in revised form 16 May 2018
Accepted 19 May 2018
Available online xxxx

Keywords:
Transmission electron microscopy
Irradiation
Creep
Zirconium
Dislocation

ABSTRACT

We report an original experimental study on a zirconium alloy deformed in situ under ion irradiation and applied stress inside a Transmission Electron Microscope. We observe that dislocations initially pinned on irradiation defects can be unpinned and glide at a lower stress under the effect of the irradiation. It is proposed that unpinning occurs by a local effect of the displacement cascade created by the incoming ion in the vicinity of the pinning point. This novel mechanism of dislocation glide assisted by irradiation is thought to play a crucial role on in-reactor irradiation creep of zirconium alloys.

During the early 60's, the irradiation creep, a visco-plastic deformation phenomenon occurring under small constant load and long term irradiation, was discovered on structural materials used in the first nuclear reactors [1–4]. As austenitic stainless steels and zirconium alloys became the most used structural materials for this application, many experimental results were available. Creep parameters, such as the stress exponent, the flux exponent and the irradiation creep activation energy were measured [5–11]. Based on these data, many theoretical mechanisms were proposed to explain the in-reactor behavior [12–19]. However very few microscopic experimental evidence [20] were available to assess which is the elementary deformation mechanism controlling irradiation creep. Despite recent efforts using advanced micro-scale testing devices under ion irradiation [21–25], there is still no clear knowledge and understanding of such mechanism.

As pointed out in Ref. [18], irradiation has two antagonistic effects on deformation creep. The first one is an inhibition of thermal creep mechanisms due to the creation of a high density of point defect clusters, in the form of small dislocation loops, acting as obstacles against dislocation glide and climb. This irradiation-retarded creep can be clearly evidenced when creep tests are conducted after irradiation or under a low neutron flux. It is related to the irradiation induced hardening. The second effect of irradiation is, on the contrary, to enhance, or even induce, creep. Indeed, it is often observed that under high neutron flux, the creep rate is higher than during out-of-pile tests. Many mechanisms have been proposed to explain this surprising phenomenon and they all involve the production of vacancies and self-interstitials under irradiation. However, these mechanisms differ in their descriptions of the fate of these point defects. Some theoretical mechanisms postulate that irradiation creep is induced solely by dislocation climb due to a biased absorption of point defects by dislocations under stress. Other proposed irradiation creep mechanisms are based on an enhanced climb-glide of dislocations by absorption of point defects under irradiation [18].

In order to assess these deformation mechanisms, we performed an experimental study using in-situ ion irradiation under an applied stress inside a Transmission Electron Microscope (TEM). This technique allows the direct observation of elementary mechanisms in real-time and at the nanometer scale. Very few attempts of this kind can be found in the literature [26–29].

The experiments were performed in the Intermediate Voltage Electron Microscope (IVEM) facility at the Argonne National Laboratory [30]. An ion beam implanter is directly connected with a TEM. The ion beam can be blanked, allowing observations under and out irradiation. Irradiations were performed using 1 MeV Kr^{2+} ions and a flux of 6×10^{14} $ions\cdot m^{-2}\cdot s^{-1}$. The final fluences ranged between 1 and 3×10^{18} $ions\cdot m^{-2}$.

Small tensile test specimens, with electron transparent areas, were taken out of a sheet of a recrystallized zirconium alloy referred to as Zircaloy-4. Details concerning this material and the sample preparation can be found in Supplementary data. The samples were installed on a GATAN single tilt heating and straining holder (Fig. 1). The deformation

* Corresponding author.
E-mail address: fabien.onimus@cea.fr (F. Onimus).

https://doi.org/10.1016/j.scriptamat.2018.05.030
1359-6462/

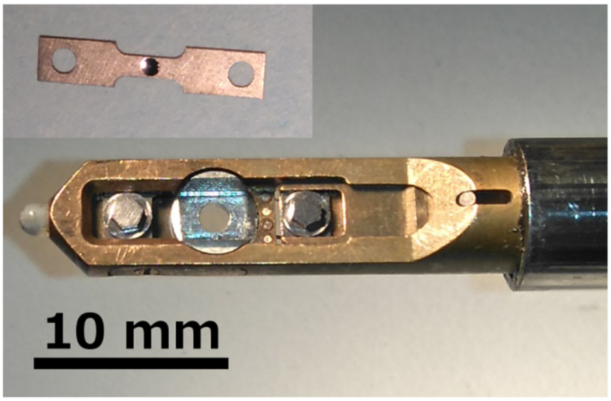

Fig. 1. Head of the heating and straining GATAN TEM sample holder. Encapsulated is shown the dog-bone shape sample used for the in situ straining experiments.

of the specimen is obtained by applying a controlled displacement of one of the grip. Observations were made in the early stages of plastic deformation by reaching a critical displacement value where first dislocation motions were noticed. During the experiment, because of the overall dislocation motion, the stress is progressively relaxed. The experiments were performed at room temperature and at temperatures ranging from 350 to 450 °C thanks to a furnace located below the sample. Samples were irradiated during several periods of few tens of seconds. When no more dislocation motion was observed, either during or out irradiation, a further slight increase of the displacement was applied. Most of the observations of dislocation motion were made after a short period of irradiation.

The motion of more than 40 dislocations in 16 different grains in several samples was analyzed. The major finding is that all the dislocations observed under applied stress were progressively pinned by the irradiation defects, when the ion beam was switched off. When the ion beam was switched on, the dislocations started to move, under irradiation, until the beam was switched off again. This stop-and-go motion was reproduced several times in all the experiments conducted.

To illustrate this phenomenon, one experiment, performed at 380 °C ± 30 °C, is described and analyzed in the following. The irradiation sequence is explained in Fig. 2 with a plot of the irradiation flux as a function of time. It is composed of irradiation periods, at constant flux of 6×10^{14} ions·m^{-2}·s^{-1}, noted B, D, F and periods when the ion beam was off noted A, C and E. This sequence was obtained after a short irradiation period of 0.13×10^{18} ions·m^{-2}. A film showing part of this sequence, accelerated two times, is provided as Supplementary data.

To analyse this sequence, the image difference technique [31] was used (Fig. 3). The image A).a) of Fig. 3 illustrates the dislocation at a time defined as $t = 0$ s and the image A).b) shows the same dislocation at $t = 20$ s. The image difference a)–b) exhibits a uniform grey contrast proving that the dislocation did not move between these two images, pinned by small irradiation loops. The images B).a) and B).b) show the glide of the dislocation under irradiation. The dislocation moves by successive rapid jumps and stops, presumably due to the pinning and unpinning of the dislocation, under the combined effect of stress and irradiation. During this period (B) the dislocation mean velocity is 17 nm·s^{-1}. After 18 s, the irradiation beam is switched off (C). The images difference C).a) shows that the dislocation still glides, during 49 s at a lower mean velocity of 8 nm·s^{-1}. Then, the dislocation stops as illustrated by the image difference on fig. C).b). The ion beam is left off during 68 s to make sure that the dislocation is stopped. As soon as the second irradiation period (D) starts the dislocation almost instantaneously glides (images difference D).a)). When the beam is again switched off the dislocation stops again (Fig. 3.E), and so on. During the irradiation periods, the dislocation motion occurs by successive fast jumps interrupted by longer stops. The waiting time (t_w) was analyzed for 9 stops. It ranges from 1 to 11 s, with a mean waiting time of 6 s. Comparatively, the jumping time was very short, less than the time between two frames, i.e. 0.1 s.

The crystal orientation of the grain was determined using electron diffraction. Based on the slip traces left by the dislocations on the surface, the glide plane was found to be the $(01\bar{1}1)$ pyramidal plane, the Burgers vector of the dislocation being $\boldsymbol{b} = 1/3[\bar{2}110]$. The gliding dislocation observed has thus a screw character. More details can be found in Supplementary data.

Experiments performed at room temperature show similar results except that a lower dislocation velocity of 2 to 4 nm·s^{-1} was measured. This observation indicates that the deformation mechanism is only slightly thermally activated and does not require a high point defect mobility, in agreement with the low activation energy often measured for irradiation creep behaviours. A film showing the dislocation motion at room temperature, accelerated two times, can be found in the Supplementary data.

The role of irradiation on dislocations originally gliding in unirradiated samples was also investigated at temperatures ranging from 350 to 450 °C. For that purpose, the sample was first strained prior to irradiation and dislocation motion was observed. During the dislocation motion, the ion beam was switched on. Irradiation defects appeared in the specimen and the dislocation progressively stopped. To compensate for the possible stress relaxation, the displacement was increased. But despite this stress increase the dislocation did not glide again. For a high enough applied displacement without the ion beam, new dislocations, presumably originating from grain boundaries, were observed to glide, with difficulty, through the irradiation defects. The observation of the pinning of originally gliding dislocations results from their interaction with irradiation defects and may explain the irradiation induced hardening and the irradiation-retarded creep previously described. It is believed that initial dislocations were pinned by large jogs formed during a long time irradiation after they stopped. On the contrary, new dislocations formed at grain boundaries are presumably less jogged

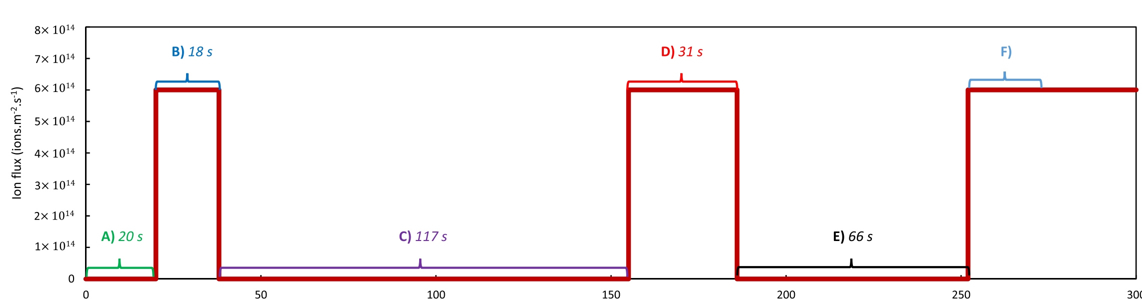

Fig. 2. Irradiation steps during the in-situ irradiation experiment using 1 MeV Kr^{2+} ion at a temperature of 380 °C ± 30 °C.

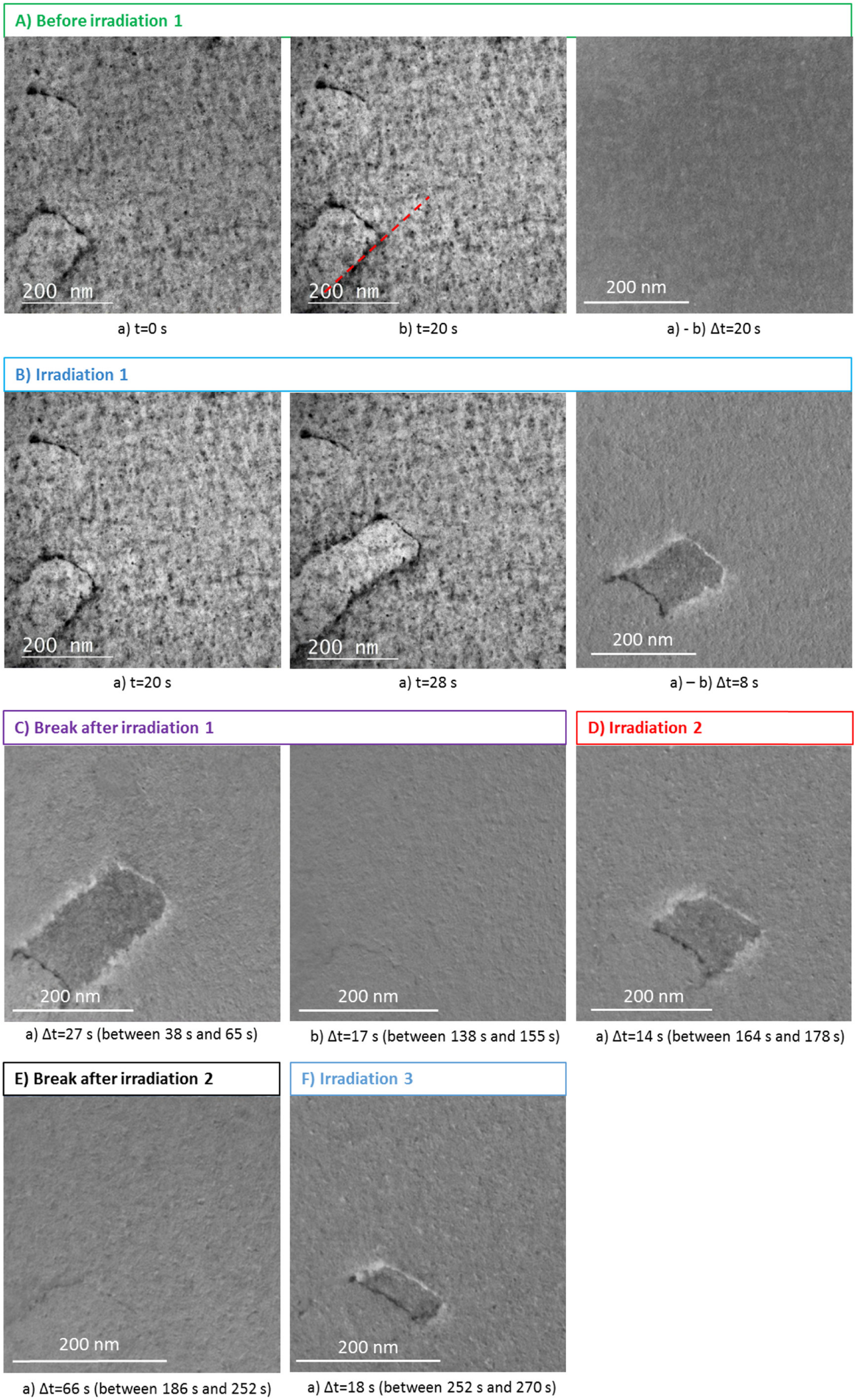

Fig. 3. Motion of a screw dislocation gliding in a pyramidal plane under 1 MeV Kr^{2+} irradiation for a temperature of 380 °C ± 30 °C and for a flux of 6×10^{14} ions·m^{-2}·s^{-1}.

and thus are able to be unpinned more easily. The activation of new dislocation sources at a larger stress level explains the irradiation-retarded creep associated to a hardening. This observation is in good agreement with what was observed in austenitic stainless steels by Briceno et al. [29].

The experiments have been able to reveal in-situ that the dislocation glide is activated by irradiation under an applied stress. Other experimental studies [32,33], where the temperature of an irradiated sample can be accurately measured under the beam, show that, in our conditions, the heating of the specimen due to the power deposited by the ion beam should be negligible. This conclusion, also supported by analytical estimation of the heat fluxes on the sample (see Supplementary data), demonstrates that the dislocation motion under stress, activated by the ion beam, is not the result of a global heating of the sample but is a direct consequence of irradiation.

In the past, many different irradiation creep deformation mechanisms were proposed. Some of them postulate that the strain results from dislocation climb due to a biased absorption of point defects under an applied stress. Our experiments show a complete different picture, where dislocations move by glide through an array of irradiation induced defects, such as dislocation loops, and dislocations are unpinned by irradiation. This mechanism bears some similarities with the one described in Ref. [34]. These new observations thus discount the deformation mechanisms based solely on dislocation climb. They also highlight the important role of the pinning and unpinning of dislocation on irradiation defects as the controlling mechanism of irradiation creep. Nevertheless, as the observations were performed close to the yield stress where the first dislocation motions were observed, the identified deformation mechanism must be regarded as a high stress irradiation creep deformation mechanism.

The details of the unpinning process are not known. It could be due to the local absorption of point defects on obstacles allowing the local climb of the dislocation leading to its release. It could also be due to the direct effect of the displacement cascade that unpins the dislocation if the displacement cascade is close enough to the pinning point. The unpinning process can be analyzed in more details by considering that individual dislocations interact with loops separated, in the dislocation glide plane, on average by a distance l. The average distance between loops in a plane can be estimated as $l \approx 1/\sqrt{Nd}$, with N the loop number density and d the mean loop diameter. As the measured loop density is $N = 1\times10^{22}\ \mathrm{m}^{-3}$ and the mean loop diameter is close to $d=10$ nm, the mean distance between loops in the dislocation glide plane is found to be 100 nm. Considering that the flying time between obstacles is negligible compared to the mean waiting time ($t_w=6$ s at 380 °C), this leads to a dislocation velocity ($\overline{v} = l/t_w$) of 17 nm·s^{-1}, in agreement with the mean velocity measured. Because the thin foil thickness is of the order of the value of l, the observations made in this study correspond to the situation where the dislocation is pinned by one obstacle between two jumps, as depicted schematically in Fig. 4.

The dislocation motion is characterized by jumps followed by waiting times, of various durations, on single pinning points. This suggests, considering that obstacles are equivalently strong, that the unpinning mechanism is a direct consequence of the interaction between cascades and pinning point, and thus is related to the random nature of the distribution of ions hitting the sample surface. It is possible to evaluate the mean effective interaction distance (r_{eff}) between an incoming ion and the pinning point. A first simple estimation can be obtained by Eq. (1) where φ is the ion flux and $\pi(r_{eff})^2$ is an interaction cross-section between the incoming particle and the pinning point. The inverse of this cross section times the ion flux is thus equal to the mean time between two ion hits reaching this area, neglecting the random nature of the particle flux.

$$\varphi\pi(r_{eff})^2 = 1/t_w \tag{1}$$

Using the mean waiting time of 6 s at 380 °C and considering that the shorter and the longer waiting times measured are 1 s and 11 s, the

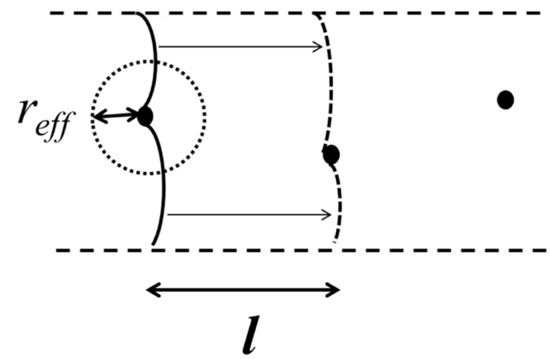

Fig. 4. A dislocation pinned on a loop is unpinned when an incoming ion falls within a disk of radius r_{eff} around the pinning point. The dislocation then jumps up to the next pinning point.

mean effective interaction distance (r_{eff}) between the particle and the pinning point is 9.4 nm, with a minimum value of 7 nm and a maximum value of 23 nm. The scatter in waiting time reflects the combined effects of the stochastic nature of the incoming ion beam, the variability in obstacle strength and also the random distribution of obstacles in the volume of the thin foil.

At room temperature a mean waiting time of 25 s is measured. The mean effective interaction distance (r_{eff}) is 4.6 nm in that case.

A more thorough statistical treatment, taking into account the random distribution of ion hits on the sample surface, can be obtained by considering that during the waiting time t_w, n ions hit a disk of unit radius ($R = 1$) with $n = \varphi t_w \pi R^2 = \varphi t_w \pi$. The probability p that one of these ions falls within the area of radius r is equal to $p = \frac{\pi r^2}{\pi R^2} = r^2$. The probability that n ions fall at a distance larger than r from the pinning point is $(1 - r^2)^n$. The average distance between the ion hits and the pinning point, which corresponds to the expected value and to the effective interaction distance, is then given by Eq. (2).

$$r_{eff} = \int_0^1 \left(1-r^2\right)^n dr = \frac{\sqrt{\pi}}{2}\frac{\Gamma(n+1)}{\Gamma(n+1.5)} \tag{2}$$

where $\Gamma(n)$ is the gamma function. With the same parameters as previously, the values of the effective interaction radius at 380 °C and room temperature are respectively 8.3 and 4.1 nm.

The fact that these values are of the order of the size of the irradiation loops, i.e. the size of the pinning points, gives credit to the hypothesis that the unpinning mechanism operates directly on the pinning point itself.

This unpinning could be either achieved by the local climb of the dislocation, around the pinning point, thanks to the absorption of point defects or by the direct effect of the displacement cascade on the pinning point, without the need for point defect diffusion. Indeed, molecular dynamics simulations have recently shown [35] that the formation of a displacement cascade close to a screw dislocation could promote its cross-slip leading to its release from the pinning point, in agreement with the mechanism observed in this present work.

It is also worth pointing out that with the mechanism proposed, the strain rate, which is proportional to the mean dislocation velocity, is thus proportional to the ion flux (Eq. (1)), as usually observed during macroscopic irradiation creep experiments. Furthermore, according to the work done in Ref. [34], a linear stress dependence arises, in the low stress regime, from a mechanism of pinning-unpinning, in good agreement with most of macroscopic experiments. This shows that the proposed mechanism, based on microscopic observation, is compatible with macroscopic measurements.

This original experimental work provides a new insight on the irradiation creep deformation of zirconium alloys under relatively high applied stress. It is observed that deformation occurs by glide of dislocations that are pinned by small loops. The dislocations are released from their pinning points by irradiation. It is proposed that when a displacement cascade is created by the incoming ion close enough to the pinning point, the dislocation is released.

Supplementary data to this article can be found online at https://doi.org/10.1016/j.scriptamat.2018.05.030.

Acknowledgements

This work used resources of the IVEM-Tandem Facility at the Argonne National Laboratory, supported by the U.S. Department of Energy, Office of Nuclear Energy under DOE Idaho Operations Office Contract DE-AC07-051D14517 as part of a Nuclear Science User Facilities experiment. The authors are grateful to the IVEM staff for helping in the experiment. The authors also want to thank EDF and Framatome for the financial support of this study.

References

[1] G.W. Lewthwaite, D. Mosedale, I.R. Ward, Nature 216 (5114) (1967) 472.
[2] R. Taylor, A.T. Jeffs, J. Nucl. Mater. 19 (2) (1966) 142.
[3] D. Mosedale, J. Appl. Phys. 33 (10) (1962) 3142.
[4] R.V. Hesketh, Philos. Mag. 8 (92) (1963) 1321.
[5] V. Fidleris, J. Nucl. Mater. 26 (1) (1968) 51.
[6] S.R. MacEwen, V. Fidleris, Philos. Mag. 31 (5) (1975) 1149.
[7] S.R. MacEwen, V. Fidleris, J. Nucl. Mater. 65 (1977) 250.
[8] A.R. Causey, F.J. Butcher, S.A. Donohue, J. Nucl. Mater. 159 (1988) 101.
[9] V. Fidleris, J. Nucl. Mater. 159 (1988) 22.
[10] A. Soniak, N. L'Hullier, J.P. Mardon, V. Rebeyrolle, P. Bouffioux, C. Bernaudat, in: G.D. Moan, P. Rudling (Eds.), Zirconium in the Nuclear Industry: Thirteenth International Symposium, ASTM STP 1423, ASTM International, West Conshohocken, PA 2002, pp. 837–862.
[11] R.A. Holt, J. Nucl. Mater. 372 (2) (2008) 182.
[12] F.A. Nichols, J. Nucl. Mater. 37 (1) (1970) 59.
[13] A.D. Brailsford, R. Bullough, Philos. Mag. 27 (1) (1973) 49.
[14] P.T. Heald, M.V. Speight, Philos. Mag. 29 (5) (1974) 1075.
[15] C. Dollins, F. Nichols, in: J. Schemel, H. Rosenbaum (Eds.), Zirconium in Nuclear Applications, ASTM STP 551, ASTM International, West Conshohocken, PA 1974, pp. 229–248.
[16] J. Gittus, Creep, Viscoelasticity, and Creep Fracture in Solids, Applied Science Publishers Ltd, England, 1975.
[17] L.K. Mansur, Philos. Mag. A 39 (4) (1979) 497.
[18] D.G. Franklin, G.E. Lucas, A.L. Bement, Creep of Zirconium Alloys in Nuclear Reactors, ASTM STP 815, ASTM International, Philadephia, PA, 1983.
[19] J.R. Matthews, M.W. Finnis, J. Nucl. Mater. 159 (1988) 257.
[20] F.A. Garner, D.S. Gelles, J. Nucl. Mater. 159 (1988) 286.
[21] K. Tai, R.S. Averback, P. Bellon, Y. Ashkenazy, Scr. Mater. 65 (2) (2011) 163.
[22] S. Özerinç, R.S. Averback, W.P. King, J. Nucl. Mater. 451 (1–3) (2014) 104.
[23] P. Lapouge, F. Onimus, R. Vayrette, J.P. Raskin, T. Pardoen, Y. Bréchet, J. Nucl. Mater. 476 (2016) 20.
[24] P. Lapouge, F. Onimus, M. Coulombier, J.P. Raskin, T. Pardoen, Y. Bréchet, Acta Mater. 131 (2017) 77.
[25] G.S. Jawaharram, P.M. Price, C.M. Barr, K. Hattar, R.S. Averback, S.J. Dillon, Scr. Mater. 148 (2018).
[26] D. Caillard, J.L. Martin, B. Jouffrey, Acta Metall. 28 (8) (1980) 1059.
[27] H. Saka, K. Kawamura, Y. Morozumi, H. Teshima, J. Nucl. Mater. 179 (1991) 966.
[28] M. Suzuki, A. Sato, J. Nucl. Mater. 172 (1) (1990) 97.
[29] M. Briceño, J. Fenske, M. Dadfarnia, P. Sofronis, I.M. Robertson, J. Nucl. Mater. 409 (1) (2011) 18.
[30] R.C. Birtcher, M.A. Kirk, K. Furuya, G.R. Lumpkin, M.O. Ruault, J. Mater. Res. 20 (7) (2005) 1654.
[31] D. Caillard, Acta Mater. 58 (9) (2010) 3493.
[32] R.E. de Lamaestre, H. Bernas, Nucl. Instrum. Methods Phys. Res., Sect. B 257 (1–2) (2007) 1.
[33] R.E. de Lamaestre, H. Béa, H. Bernas, J. Belloni, J.L. Marignier, Phys. Rev. B 76 (20) (2007), 205431. .
[34] B.T. Kelly, A.J.E. Foreman, Carbon 12 (2) (1974) 151.
[35] R.E. Voskoboinikov, Nucl. Instrum. Methods Phys. Res., Sect. B 303 (2013) 104.